

Reaction Mechanism | Very Important Paper |

VIP Unprecedented Mechanism of an Organocatalytic Route to Conjugated Enynes with a Junction to Cyclic Nitronates

Verena Streitferdt,^[a] Michael H. Haindl,^[a] Johnny Hioe,^[a] Fabio Morana,^[a] Polyssena Renzi,^[a] Felicitas von Rekowski,^[a] Alexander Zimmermann,^[a] Martina Nardi,^[a] Kirsten Zeitler,^[a,b] and Ruth M. Gschwind^{*[a]}

Abstract: Conjugated enynes as well as cyclic nitronates are crucial building blocks for numerous natural products and pharmaceuticals. However, so far, no common and metal-free synthetic route to both conjugated enynes and cyclic nitronates has been reported. Herein, in situ NMR, labelling studies and theoretical calculations were combined to investigate the mechanism of the unusual triple bond formation towards conjugated enynes. Starting from nitroalkene dimers, first an isoxazolidine-2,5-diol derivative is formed as central intermediate. From this, enynes were generated by a combination of oxid-

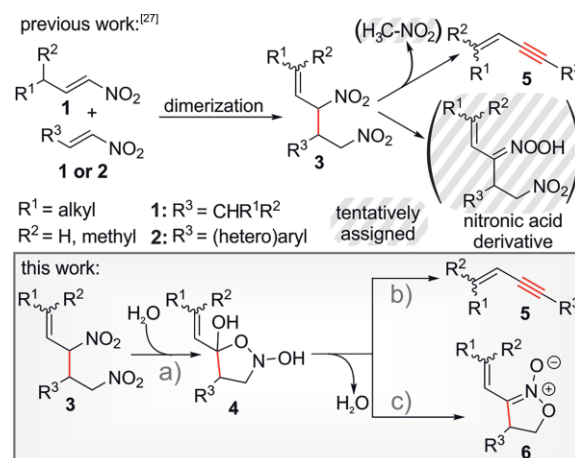
ation, dehydration, and retro 1,3-dipolar cycloaddition, whereas for nitronates a base induced intramolecular reorganization is proposed. While the product distribution could be controlled and high yields of nitronate were achieved, only medium to good yields for enynes were obtained due to polymerization losses. Nevertheless, we hope that these mechanistic investigations may provide a basis for further developments of organocatalytic or metal-free preparations of conjugated enynes and nitronates.

Introduction

In the fields of natural products and drug design, nitronates and conjugated enynes are valuable building blocks. While the structural motif of a conjugated enyne occurs in many pharmaceuticals and natural compounds [e.g. Dynemicin A,^[1] Terbinafine^[2,3] (Lamisil®), callipeltosides^[4] or Neocarzinostatin^[5]], nitronates, especially cyclic nitronates, find application in the synthesis of biologically active compounds,^[6,7] drug candidates^[8–10] and natural products.^[11] Due to the fundamental structural dissimilarities between cyclic nitronates and conjugated enynes, these compounds are generally accessed by disparate strategies. The most established methods for the formation of conjugated enynes are metal catalyzed cross-couplings exploiting the presence of double and triple bonds in the starting materials.^[3,12–17] Although metal-free procedures, especially organocatalytic ones, to conjugated enynes would be very valuable, they are rarely found in literature.^[18] On the other hand, numerous metal-free procedures for the synthesis of cyclic nitronates already exist among which intramolecular cyclization via substitution and cycloadditions are commonly employed.^[19] Despite their structural divergences, conjugated enynes and nitronates exhibit common reactivities. The zwitterionic structure of nitronates allows them to react as α -C-electrophiles, but

also as ambident nucleophiles due to their O- and α -C-nucleophilicity.^[19] Moreover, nitronates are 1,3-dipoles and thus can inter alia participate in [3+2]-cycloadditions generating highly functionalized heterocycles.^[19] Similar to nitronates, also conjugated enynes can partake in cycloadditions.^[20] Furthermore, they can be subjected to other ring-closing^[21,22] and coupling reactions,^[23,24] or they can serve as transition metal ligands.^[25]

A few years ago, in our working group Markus Schmid discovered the first organocatalytic route to conjugated enynes, in which the C–C triple bond is constituted out of a C–C single



Scheme 1. General reaction scheme to conjugated enyne 5 and cyclic nitronate 6 from nitroalkenes 1 and 2 or dimer 3 via linking intermediate 4. The mechanism starting from dimer 3, highlighted by a gray frame, is elucidated in this work: a) cyclization of dimer 3 to intermediate 4; b) fragmentation of 4 to conjugated enyne 5; c) rearrangement of 4 to cyclic nitronates 6.

[a] Faculty of Chemistry and Pharmacy, University of Regensburg, Universitätsstr. 31, 93053 Regensburg, Germany
E-mail: Ruth.Gschwind@ur.de
<http://www-oc.chemie.uni-regensburg.de/gschwind/>

[b] Institute of Organic Chemistry, University of Leipzig, Johannisallee 29, 04103 Leipzig, Germany

Supporting information and ORCID(s) from the author(s) for this article are available on the WWW under <https://doi.org/10.1002/ejoc.201801153>.

bond in a one-pot reaction.^[26] Starting from α,β -unsaturated nitroalkenes **1** and **2** with proline-based catalysts, first nitroalkene dimers **3** were generated via a *Rauhut-Currier*-like reaction^[27–29] (see Scheme 1 top) followed by the fragmentation to conjugated enynes.^[26] Furthermore, the pronounced formation of another product was observed, which could be suppressed upon addition of benzoic acid and was tentatively assigned to a nitronic acid derivative.^[26]

However, the mechanism of this unprecedented fragmentation as well as the nature of the other product remained unclear. The postulated mechanism via fragmentation to enyne and nitromethane was regarded to be improbable, because nitromethane did not accumulate during the reaction in the expected amount.^[26]

Herein, we present our profound mechanistic study on the unusual organocatalytic formation of conjugated enynes by means of NMR in combination with theoretical calculations. The product generated alongside the enyne could be identified as a cyclic nitronate. In addition, an unprecedented cyclic intermediate **4** was discovered, which was found to be common to the mechanistic pathways of both conjugated enyne **5** and cyclic nitronate **6** (see Scheme 1 bottom). Furthermore, ¹³C and ¹⁵N labelling studies allowed for the identification of N₂ and CO₂ as fragmentation byproducts in the enyne formation. Hence, a comprehensive mechanism for the first combined metal-free synthesis of conjugated enynes and cyclic nitronates is proposed. A retro-1,3-dipolar cycloaddition as a fragmentation towards the enyne as well as complex intramolecular rearrangements towards the nitronate are postulated. In addition, factors influencing the product outcome are identified and approaches to modify this outcome are presented.

Results and Discussion

Compound Pool for Mechanistic Studies. While the dimerization of nitroalkenes follows the expected *Rauhut-Currier*-type mechanism,^[26,27] the mechanistic pathway to conjugated enynes was still unsettled. Therefore, we focused our NMR study on the mechanism and intermediates downstream to nitroalkene dimers. As starting material for our studies dimer **3a**, synthesized from the unsubstituted nitropentene **1a**, was selected to allow investigations on double bond isomerization, while dimers **3b–c** were chosen to examine electronic effects (see Figure 1a; for syntheses see SI). ¹⁵N labeled dimer **3a¹⁵N** was used for structural investigations on intermediate **4** during in situ NMR reaction monitoring. For the investigation of the fragmentation byproducts by ¹⁵N and ¹³C labeling, one-pot reactions were applied to avoid compound loss by further conversion to the dimer (see Figure 1a, **1a¹⁵N** and **1a¹³C**). Various bases, acids or their combinations were examined (see Figure 1c–d, for further catalyst screening see SI), since the initial studies revealed that the reaction to both enyne and nitronate requires a base.^[26] Acids as additional additives potentially suppress the formation of nitronates.^[26] An NMR solvent screening including DMSO, DMF, methanol, benzene, dioxane, nitromethane, dichloromethane and acetonitrile revealed that highest yields were obtained in DMSO (for more information see SI). There-

fore, hereafter exclusively the studies in [D₆]DMSO are discussed. Consequently, in Figure 1c–d the pK_a values are given in DMSO as far as available. Otherwise, pK_a values in water are provided.

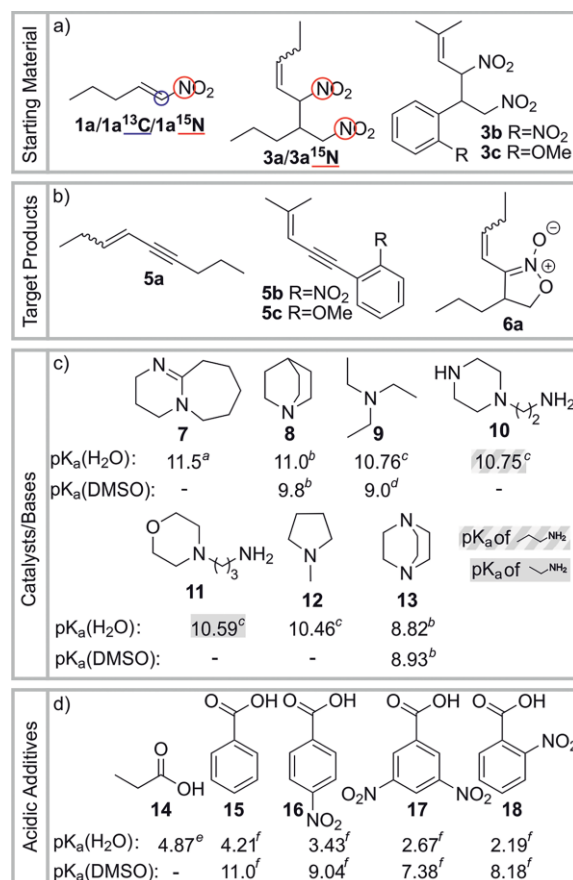


Figure 1. Model substrates for the mechanistic investigation of the reaction to conjugated enynes **5a–c** and cyclic nitronate **6a**; atoms marked in blue and red were labelled with ¹³C and ¹⁵N, respectively; pK_a values are given at 25 °C: aⁱ,^[30] bⁱ,^[31] cⁱ,^[32] dⁱ,^[33] eⁱ,^[34] fⁱ,^[35] for syntheses see SI.

Overall, no significant mechanistic deviations were found for one-pot reactions and those starting from dimers regarding intermediate species (outcome and product distribution was dependent on solvent and reaction conditions). Therefore, the information of both reaction types could be combined.

Identification of Cyclic Nitronate as Second Product. Parallel to the formation of **5**, the generation of a side product was observed.^[26] Characterization of this side product by 2D NMR spectroscopy and mass spectrometry revealed this compound not as the originally suspected nitronic acid derivative,^[26] but as the cyclic nitronate **6a**. The structure of **6a** could be further confirmed by removal of the exocyclic oxygen by P(OCH₃)₃^[36] and thereby reducing **6a** to the corresponding cyclic O-alkyl-oxime (see SI). The highest yield of **6a** (84 %) was obtained with the base triazabicyclodecene (for synthesis and chemical assignment of **6a** see SI).

Common Pathway of Nitronates and Enynes to a Central Linking Intermediate. Applying nitroalkene dimers as starting material, NMR reaction monitoring revealed the formation of a new intermediate **4** (see Scheme 1 bottom) in the initial phase

of the reaction. The detectable concentration of intermediate **4** highly depends on the base strength (see Figure 2). This is shown on the reaction profiles of **3a** with DBU **7** and quinuclidine **8** (Figure 2b). Applying DBU as base, dimer **3a** was instantly and nearly completely converted to intermediate **4a** (10 % *E*-isomer and 83 % *Z*-isomer, see Figure 2a). Employing quinuclidine **8** as base generated significantly smaller amounts of **4a** (initial 30 %). The application of further bases corroborated the trend, that stronger bases generate higher amounts of **4** (see Figure 4 in SI). In addition, the type and strength of base affect significantly the product distribution between enynes and nitronates. With DBU about 60 % nitronate **6a** and 9 % of enyne **5a** was formed, while in presence of the less basic quinuclidine, enyne **5a** was the major product with 29 % yield and only 10 % of nitronate **6a** was generated. Furthermore, mechanistic investigations of the nitronate formation showed a clear correlation between the basicity, yield and formation rate of nitronate (see section "Selectivity" and Figure 7).

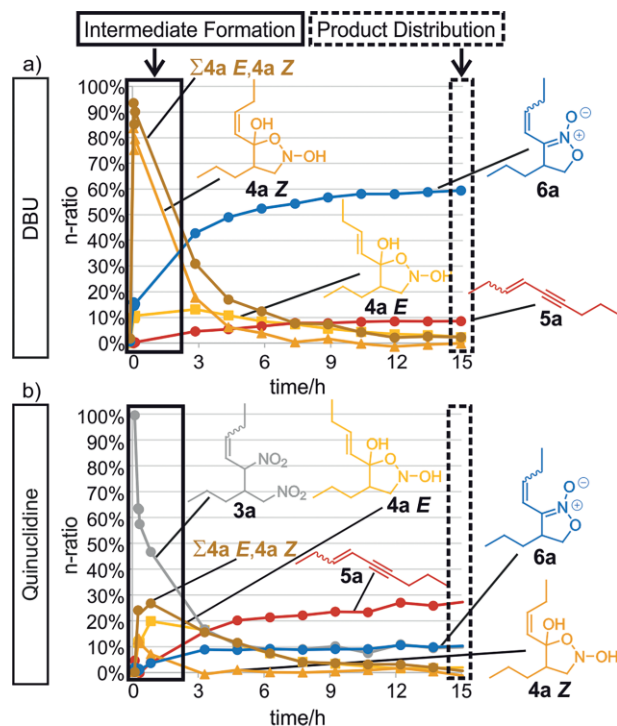


Figure 2. Base dependent formation of the central linking intermediate **4a** as precursor for both enyne and nitronate. Strong bases caused high amounts of **4a** and nitronate (a), while enynes were the main product with weaker bases (b); a) **3a** (55 mM) with DBU (82 mM) in $[D_6]DMSO$ at 298 K; b) **3a** (55 mM) with quinuclidine (82 mM) in $[D_6]DMSO$ at 298 K.

Next, the question arose, whether intermediate **4a** is part of the mechanistic pathway of both main products, enyne and nitronate. Figure 2 reveals that **4a** was present in high concentrations independent of the main product indicating that **4a** is a linking element for the formation of both enynes and nitronates. This was further corroborated by a modified experiment with DBU: Using a starting point with mainly **4a** detectable and only traces of dimer **3a** left, benzoic acid **15** was added leading to an increased amount of enyne (for data see SI). The structure of intermediate **4a** was investigated during in

situ NMR reaction monitoring, since it was too unstable for other methods. Various 2D NMR experiments were used to assign the proton and carbon spin systems of this quite unusual intermediate (see Figure 3 and SI for spectra). To identify heteroatoms and their connectivity in **4a** theoretical calculations and ^{15}N -isotope labelling were applied. 1D proton decoupled ^{13}C spectra of in situ generated **4a** ^{15}N revealed a single ^{13}C - ^{15}N coupling constant of 6.3 Hz between carbon **B** and the nitrogen, which excluded a nitrogen directly bound to the quaternary carbon **A** (see Figure 3). Theoretical calculations of 1H , and ^{13}C chemical shifts enabled to differentiate between potential arrangements of oxygen moieties in **4a** (for details see SI). The structure of **4a** fitting best to both experimental and theoretical data is displayed in Figure 3 revealing as basic structure an isoxazolidine-2,5-diol.

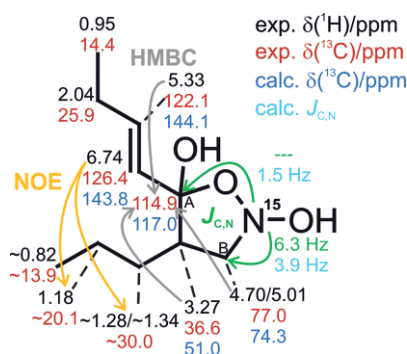
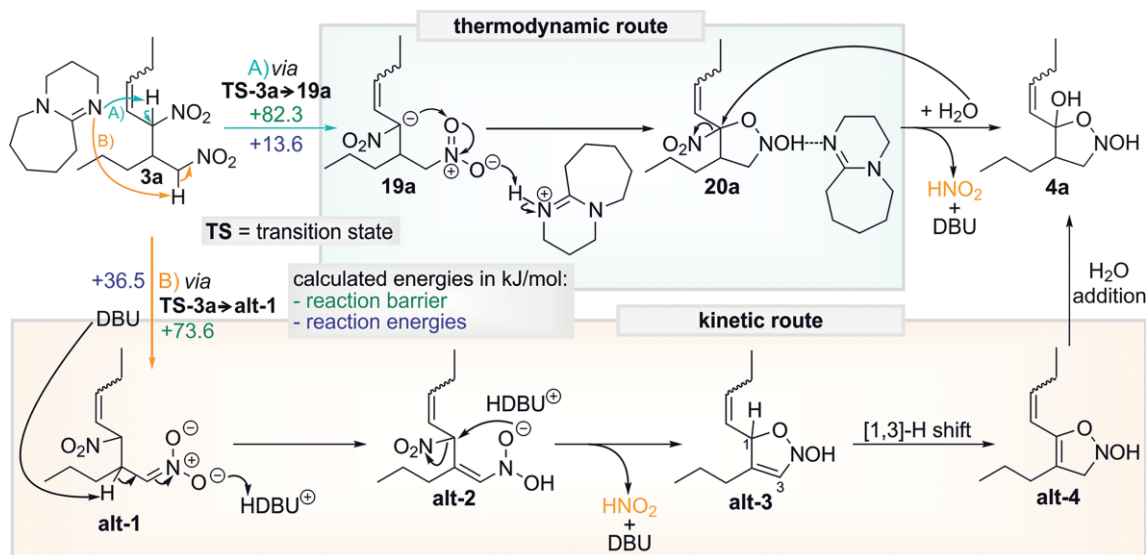


Figure 3. Structural assignment of the central linking intermediate **4** shown on **4a E**. Combined NMR and theoretical data reveal as central feature an isoxazolidine-2,5-diol (for details see text and SI).

Next, the mechanistic pathway towards linking intermediate **4** was investigated (see Scheme 2). The correlation between formation of **4** and the base strength (see Figure 2 and text above) indicates a deprotonation as the rate-determining step. Two different deprotonations of **3a** would be conceivable: in α -position to the secondary nitro group (A) and in α -position to the primary nitro group (B). Both routes were investigated with quantum chemical calculations. The energy profiles of route A with and without DBU or water reveal, after the deprotonation towards **19a**, a concerted cyclization and protonation mechanism towards **20a** (see Scheme 2). Calculations showed that free **20a** is 42.8 kJ/mol less stable than **3a**. However, coordination of DBU results in massive stabilization of **20a** by 35.3 kJ/mol compared to the base free case. Thus, the base does not serve only as de- and reprotonating agent, but also acts as stabilizer of intermediate **20a** via a hydrogen bond. Such stabilization strategy have been also utilized and observed in enamine catalysis.^[37] Furthermore, calculations showed that coordination of the conjugated acid to the primary nitro group in **19a** enables a concerted process: the attack of the carbanion on the other nitroxylic oxygen of this nitro group and the proton transfer. This indicates that in the formation of intermediate **4a** protonation of **19a** is essential for the reaction to occur. Altogether, the base facilitates the pathway towards **20a** and subsequently **4a**. Since $[D_6]DMSO$ always contains some amount of water, intermediate **20a** is expected to be transformed via an S_N reaction into **4a** upon release of HNO_2 .



Scheme 2. Proposed mechanism from dimer **3a** to linking intermediate **4a**. Theoretical calculations predicted that two pathways may lead towards **4a**: A) deprotonation in α -position to the secondary nitro group is the thermodynamically favored route over **19a** via subsequent concerted ring closure to **20a**. Substitution of the nitro group in **20a** by water generates intermediate **4a**. Our calculations revealed that DBU can stabilize **20a** and thus enables the formation of **4a**. B) Deprotonation in α -position to the primary nitro group is the kinetically favored route via nitronate **alt-1** followed by an interconversion to **alt-2** and subsequent ring closure by intramolecular substitution of the secondary nitro group to **alt-3**. Via an ensuing [1,3]-H-shift to **alt-4** and addition of water addition, intermediate **4a** may be generated.

A second alternative towards **4a** may be the abstraction of the proton in the α -position next to the primary nitro group (path B in Scheme 2). This leads to the formation of an unstable intermediate **alt-1**. Quantum chemical calculations predicted that the deprotonation of **3a** to **alt-1** is by 22.9 kJ/mol more demanding than the deprotonation leading to **19a**. On the other hand, the abstraction of the α -proton of the primary nitro group is kinetically slightly favored by 8.7 kJ/mol. Hence, the second pathway might be feasible in case **alt-1** is stabilized by the formation of hydrogen bonds to the conjugated acid (H-DBU⁺) as for **20a** to the base. Subsequently, the reactive **alt-1** probably rapidly interconverts to **alt-2** through an [1,4]-H shift, which is followed by an intramolecular ring closure to **alt-3** via the attack of the oxygen of the *N*-hydroxy-hydroxylamine releasing HNO₂. Finally, the formation of **4a** is suggested to be concluded via an [1,3]-H shift generating **alt-4** and the subsequent addition of water (for other potential mechanisms to intermediate **4** and their exclusion see SI).

Our calculations of the first reaction barriers (TS-**3a**→**19a** and TS-**3a**→**alt-1**) and reaction energies (**3a** towards **19a** and **alt-1**) revealed, that the formation of intermediate **4** may proceed via both pathways A and B. While pathway A is thermodynamically favored, pathway B is kinetically favored.

Base dependent shifts of the protons attached to the double bond in **4a** were observed (see Figure 3 in the SI). Thus, a stabilization of **4a** by hydrogen bonding to bases is highly probable similar to the situation of **20a**.

Furthermore, the NMR profiles displayed in Figure 2 indicate that partial isomerization of the double bond proceeds within the formation pathway of **4**. While the starting material **3a** consisted of 95 % *Z*-isomer and 5 % *E*-isomer, the amount of the *E*-isomer in **4a** was found to be significantly higher (10 % with DBU; 20 % with quinuclidine; see Figure 2). This isomerization

towards the energetically lower *E*-isomer may take place at the stage of the allylic anion **19a** or **alt-3** in case of deprotonation at position 1. In accordance with that, the NMR reaction profiles revealed a faster conversion of **4a** *Z* than **4a** *E* for both bases (see Figure 2).

Mechanism of the Conjugated Enyne Formation. Next, we investigated the fragmentation mechanism from intermediate **4** towards conjugated enyne **5** (see Scheme 1 bottom). Since no further intermediates could be detected, the identification of fragmentation byproducts was of most importance to get experimental evidence for discriminating other potential mechanistic pathways. The most obvious byproduct would be CH₃NO₂ via an elimination.^[26] However, accumulation of nitromethane in parallel to the product formation was never observed. Instead, in situ ¹³C NMR monitoring of the one-pot reaction of **1a**¹³C revealed the generation of ¹³CO₂ correlating directly to the formation of **5a**¹³C (see Figure 4; for further experimental confirmation of CO₂ as byproduct see SI).

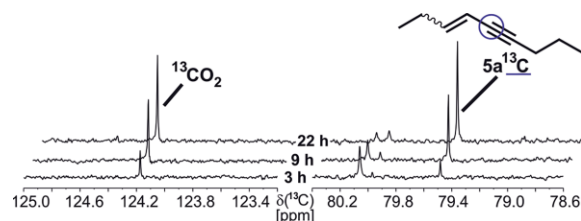


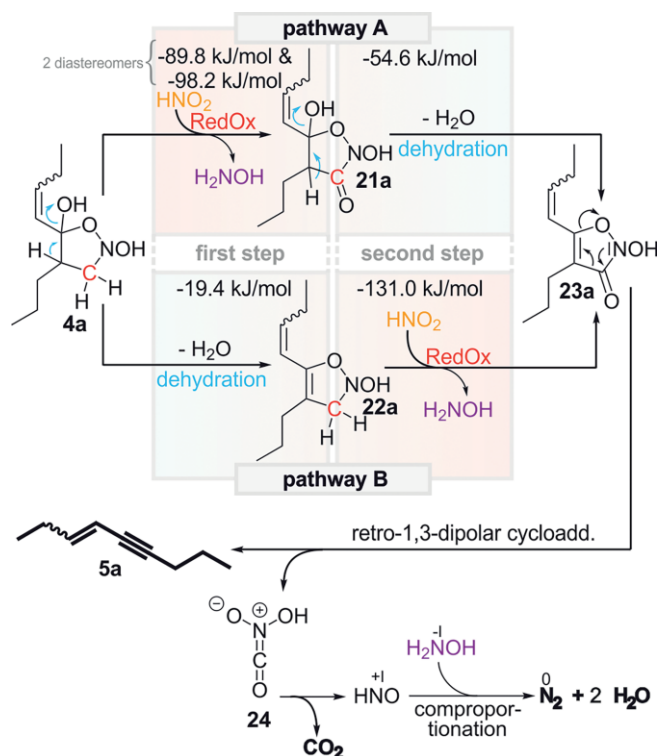
Figure 4. Correlated formation of ¹³CO₂ and enyne **5a**¹³C indicating CO₂ as fragmentation byproduct of the enyne pathway [¹³C NMR reaction monitoring of **1a**¹³C (40 mM) with diphenylprolinol (20 mM) in [D₆]DMSO at 300 K].

To elucidate the fate of the nitrogen we applied ¹⁵N NMR in situ reaction monitoring to a one-pot reaction of **1a**¹⁵N. *Inter alia* pronounced signals at δ = 310.8 ppm and 617.7 ppm ap-

peared. The chemical shift of 310.8 ppm matches well a literature value of molecular nitrogen ($\delta = 310.1$ ppm).^[38] In the initial stage of the reaction, the N_2 signal increases together with the enyne formation. After about 4 h, the signal intensities deviate most probably due to degassing effects of N_2 (for data see SI). This is, however, not the case for CO_2 probably due to its significantly higher solubility in DMSO than N_2 .^[39] The ^{15}N signal at $\delta = 617.7$ ppm is close to the literature value of sodium nitrite in water ($\delta = 608$ ppm).^[40] Considering the differences of our system in terms of solvents (DMSO vs. H_2O), counterions (Na^+ vs. H -base $^+$) and the potential presence of free HNO_2 , the signal at $\delta = 617.7$ ppm can readily be assigned to $X^+-NO_2^-$ generated in the formation of intermediate **4a** (for kinetic profile and the assignment of the other ^{15}N -signals see SI). Additionally to CO_2 and N_2 , H_2O was observed as third byproduct of the fragmentation of **4a** into enyne. During 1H NMR monitoring of reactions from **3a** to enyne **5a**, a significant increase of the water signal could be observed. Similar to CO_2 and N_2 , the water build-up correlates qualitatively with the enyne formation (for data see SI). Thus, CO_2 , N_2 and water represent byproducts in the conjugated enyne **5** formation.

Based on the experimental detection of CO_2 , N_2 and H_2O as byproducts and supported by quantum chemical calculations we propose the transformation of intermediate **4** into conjugated enyne **5** via a combination of oxidation, dehydration and retro 1,3-dipolar cycloaddition as depicted in Scheme 3. The order of oxidation (by HNO_2) and dehydration depends most likely on the experimental condition. Our theoretical calculations show that both pathways **A** and **B** depicted in Scheme 3 between **4a** and **23a** are strongly exergonic. In case **A** the oxidation occurs first and **21a** together with hydroxylamine H_2NOH are generated in an exergonic fashion (-89.8 to -98.2 kJ/mol depending on the diastereomeric starting intermediate). This is followed by the dehydration step to **23a**, which is also exergonic [$\Delta G = -54.6$ kJ/mol; dehydration of **21a**(*R,R*)] but mainly driven by the entropy ($T^*\Delta S = +53.5$ kJ/mol). In case **B**, the order is reversed. The dehydration step is significantly less exergonic compared to the first step in case **A** [$\Delta G = -19.4$ kJ/mol; dehydration of **4a**(*R,R*)]. However the substrate **22a** possesses higher oxidation potential, and therefore the subsequent step to **23a** is even more facilitated ($\Delta G = -131.0$ kJ/mol). Subsequently, we propose a fragmentation of **23a** via a retro 1,3-dipolar cycloaddition to the conjugated enyne **5a** and compound **24**, which could be described as an "oxidized nitron" (see Scheme 3). Further, we propose a Nef-type decomposition^[41,42] of the unstable side product **24** to CO_2 and HNO . HNO in turn comproportionates with the oxidation byproduct H_2NOH to N_2 and H_2O (see Scheme 3). The proposed mechanism in Scheme 3 is in accordance with all three experimentally detected byproducts CO_2 , N_2 and H_2O . Furthermore, we observed the formation of DMS in the reaction to conjugated enyne **5a** implying a reduction of the solvent DMSO (for more information see SI). This hints at the presence of redox active species corroborating the proposed redox reaction in the mechanism from **3a** to **5a** (see Scheme 3).

In agreement with our proposed mechanism, conventional nitrones are well known for forward 1,3-dipolar cycloadditions



Scheme 3. Proposed mechanism from intermediate **4a** to conjugated enyne **5a** (NMR detected compounds are bold). The oxidation step is in both pathways strongly exergonic/exothermic, while the dehydration is entropically driven and enthalpically demanding for pathway B ($\Delta H = +32.4$ kJ/mol; $\Delta G = -19.4$ kJ/mol), respectively weakly exothermic for pathway A ($\Delta H = -1.1$ kJ/mol; $\Delta G = -54.6$). Depending on the experimental conditions different combinations of oxidation and dehydration lead to intermediate **23a**. Next a retro-1,3-dipolar cycloaddition fragments **23a** to **5a** and **24**. Then **24** decomposes further to CO_2 and HNO with HNO comproportionating with H_2NOH to N_2 and water.

with terminal alkynes (see Scheme 3a in SI)^[43] via postulated cyclic five-membered rings resembling **23a**.^[44] Next, Nef-type reactions can be assumed for the decomposition of **24**, which are feasible in a wide pH range (see Scheme 3b, c in SI).^[41,42]

While the buildup of N_2 was detected (see above) as comproportionation product of HNO and H_2NOH , a degradation of HNO to N_2O ^[45,46] (see Scheme 3e in SI) was not observed in the NMR kinetic measurements of **1a** ^{^{15}N} ($^{15}N_2O$ signals should appear at around 155 ppm and 240 ppm).^[49]

Next, the effects of different acids, substituents and bases were investigated to get further insights into the mechanism of the conjugated enyne formation. A carboxylic acid as additive accelerated significantly the formation of enyne and suppressed the formation of nitronate almost completely (compare a and b). Acid as additive is considered to have two effects in the enyne mechanism. The dehydration should be facilitated and the oxidizing power of HNO_2 increased due to a lower pH. Furthermore, with electron poor compound **3b** (see Figure 1), we also observed a faster enyne **5b** formation than with the electron rich **3c** into **5c** in the presence of benzoic acid **15** as additive. This corroborates the theoretical calculations revealing the dehydration as an enthalpically demanding step (for kinetic

profiles see Figure 7 in SI). Without acidic additives, the enyne formation is in general by far slower (see Figure 5a).

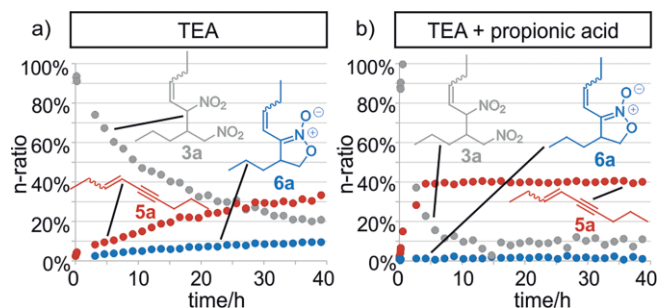
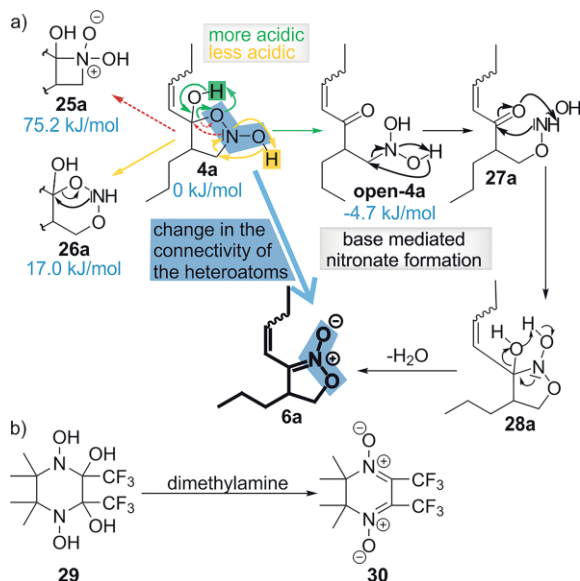


Figure 5. Acids accelerated the enyne formation and suppress nitronates. a) slow formation of **5a** and **6a** in presence of TEA 10 without acid [not completed after 40 h; **3a** (55 mM) with TEA (72 mM) in $[D_6]DMSO$ at 298 K]; b) 10-fold faster formation of **5a** and suppression of **6a** in presence of TEA with acid **14** [**3a** (55 mM) with TEA (77 mM) and propionic acid (115 mM) in $[D_6]DMSO$ at 298 K].

Mechanism of the Cyclic Nitronate Formation. Next, by applying various acidic additives as well as bases the mechanistic pathway towards nitronates **6** was examined and corroborated by theoretical calculation. Addition of carboxylic acids suppressed the nitronate formation significantly (see Figure 5 and chapter above). In accordance with that, the formation rate and yield of nitronate **6a** increased with higher pK_a values (see Figure 7; for pK_a see Figure 1). These experimental data suggest a deprotonation of intermediate **4a** as key step towards nitronates (see Scheme 4a).



Scheme 4. a) Proposed mechanism from intermediate **4a** to cyclic nitronate **6a** based on quantum chemical calculations. Relative intermediate energies of cyclic intermediates **25a** and **26a** and open chain intermediate **open-4a** indicate that the reaction most likely proceeds via **open-4a** after hemiketal opening. Further, a rearrangement of the nitrogen and oxygen atoms towards **27a** is proposed. Intramolecular ring closure is suggested to generate **28a** which leads to nitronate **6a** after dehydration; b) recently reported dehydration^[48] similar to the postulated step from **28a** to **6a**.

Since no further intermediates between **4a** and nitronate **6a** were detected experimentally, theoretical calculations were

used to compare the relative energetics of possible intermediate structures. Several possible pathways leading to **6a** were considered including the formation of cyclic intermediates **25a** and **26a** and open chain intermediate **open-4a**. Both cyclic intermediates are energetically strongly disfavored compared to intermediate **4a**. Since a significant production of nitronate **6a** in mild basic condition was observed (see a), such uphill energetic profiles to **25a** and **26a** are hence very unlikely. In contrast, the base mediated rearrangement of **4a** to the open chain intermediate **open-4a** is thermodynamically slightly favored over **4a** by 4.7 kJ/mol. Moreover, our calculations revealed that the hemiketalic proton is more acidic than the *N*-hydroxylic one. Therefore, we propose the formation of nitronate **6a** to proceed via the open chain intermediate **open-4a**. Further, we suggest a first change in heteroatom connectivity by a rearrangement of **open-4a** to **27a**. Next, we propose a reformation of the five-membered ring together with a second change of heteroatom connectivity towards intermediate **28a**. Finally, a dehydration of **28a** to cyclic nitronate **6a** is suggested. Recently, a similar dehydration step inter alia under basic conditions was reported (see Scheme 4b).^[48]

Selectivity: Conjugated Enyne vs. Cyclic Nitronate. As discussed above both products share a common mechanistic pathway to the central linking intermediate **4**, which subsequently splits towards conjugated enynes **5** and cyclic nitronates **6**. Hence, we examined factors influencing the product distribution, more precisely acidic additives, temperature and basicity.

The use of sufficient amounts of acids in addition to the base suppressed the formation of nitronate **6** down to a few percent and accelerated the generation of conjugated enyne **5** (see preceding discussion and Figure 5). In a small screening of acids benzoic acid **15** led to the fastest formation of **5a** (see Figure 6). However, stronger acids were found to be detrimental, because they in turn decelerated the enyne formation considerably (see Figure 6). This essential balance between basic and acidic experimental conditions corroborated the proposed mechanism (see Scheme 2, Scheme 3a and Scheme 4a).

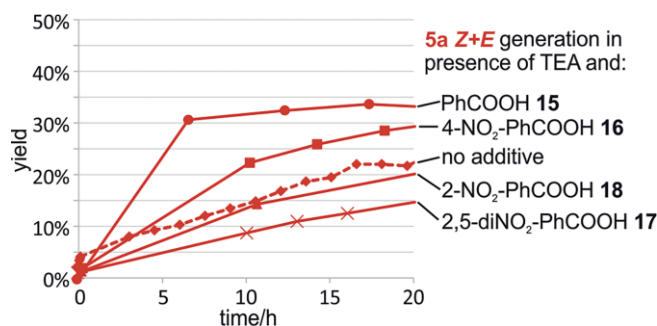


Figure 6. The stronger the acid, the slower is the enyne formation. With too strong acids **17** and **18** the reaction velocity towards enyne even falls below that in absence of acidic additive [**3a** (55 mM) with TEA (1.3 equiv.) and acid (1.3 equiv.) in $[D_6]DMSO$ at 298 K].

For the generation of the linking intermediate **4** a certain basicity is indispensable (see Scheme 2), while acids accelerate the enyne and suppress nitronate formation. Surprisingly, elevated temperatures altered this product distribution in an ex-

periment of **3a** with TEA and benzoic acid. There, at 298 K nitronate **6a** was suppressed below 3 % yield in the presence of benzoic acid. However, applying 320 K, 13 % of nitronate was produced even in presence of benzoic acid. This hints at an alternative nitronate pathway potentially involving higher energetic intermediates at elevated temperatures (for more information see SI).

Based on these results, a synthetic route to **6a** (84 %) was developed combining elevated temperature and a strong base (**3a** with triazabicyclododecene at 50 °C; for procedure see SI).

Under purely basic conditions, we also observed a rough correlation between the basicity and product distribution. While, with strong bases DBU **7** and 1-(2-aminoethyl)-piperazine **10** nitronate **6a** was clearly the major product with all other bases enyne emerged as major product (except for **11** where no enyne **5a** was generated). For the nitronates **6a**, the rates and yields increased with stronger bases (see Figure 7). For the conjugated enyne **5** no clear correlation was observed between basicity, yield and rate most probably due to the complex mechanism.

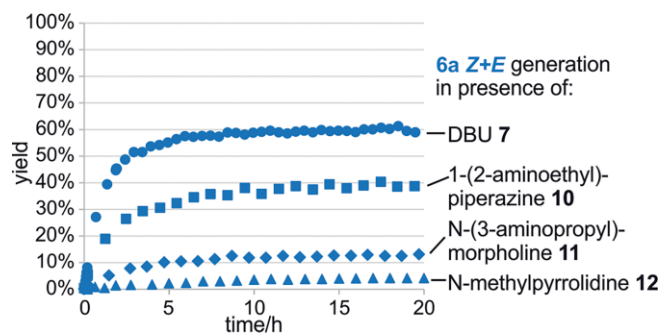


Figure 7. Strong bases lead to higher rates and yields in the formation of nitronate **6a** [**3a** (80 mM) with 1 equiv. of base respectively: DBU **7**, 1-(2-aminoethyl)piperazine **10**, N-(3-aminopropyl)morpholine **11** and N-methylpyrrolidine **12**].

Yield and scope of the combined route to conjugated enynes and cyclic nitronates. While for the synthesis of cyclic nitronates, there already exist several metal-free strategies,^[19] for conjugated enynes they are rare.^[18] Hence, we mainly focused on examining the scope of conjugated enynes **5**. We found that conjugated enynes could be generated starting from both homo- and heterodimers (derived from the dimerization of **1** with **1** or **1** with **2**) as well as directly from nitroalkenes **1** and **2** within a one-pot reaction. Besides aliphatic enyne **5a**, which was obtained in good to moderate NMR yields up to 57 %, and the aromatic enynes **5b** and **5c** several other aliphatic, heteroaromatic and functionalized/non-functionalized aromatic conjugated enynes could be generated successfully. This demonstrates a tolerance of the enyne formation towards electronically and sterically different substituted dimers **3** and nitroalkenes **1** and **2** (for scope and procedures see Figure 16 in the SI). To the cyclic nitronate formation, only aliphatic precursors were applied. Yet, higher yields were achieved up to 84 % (for scope and procedures see Figure 17 in the SI).

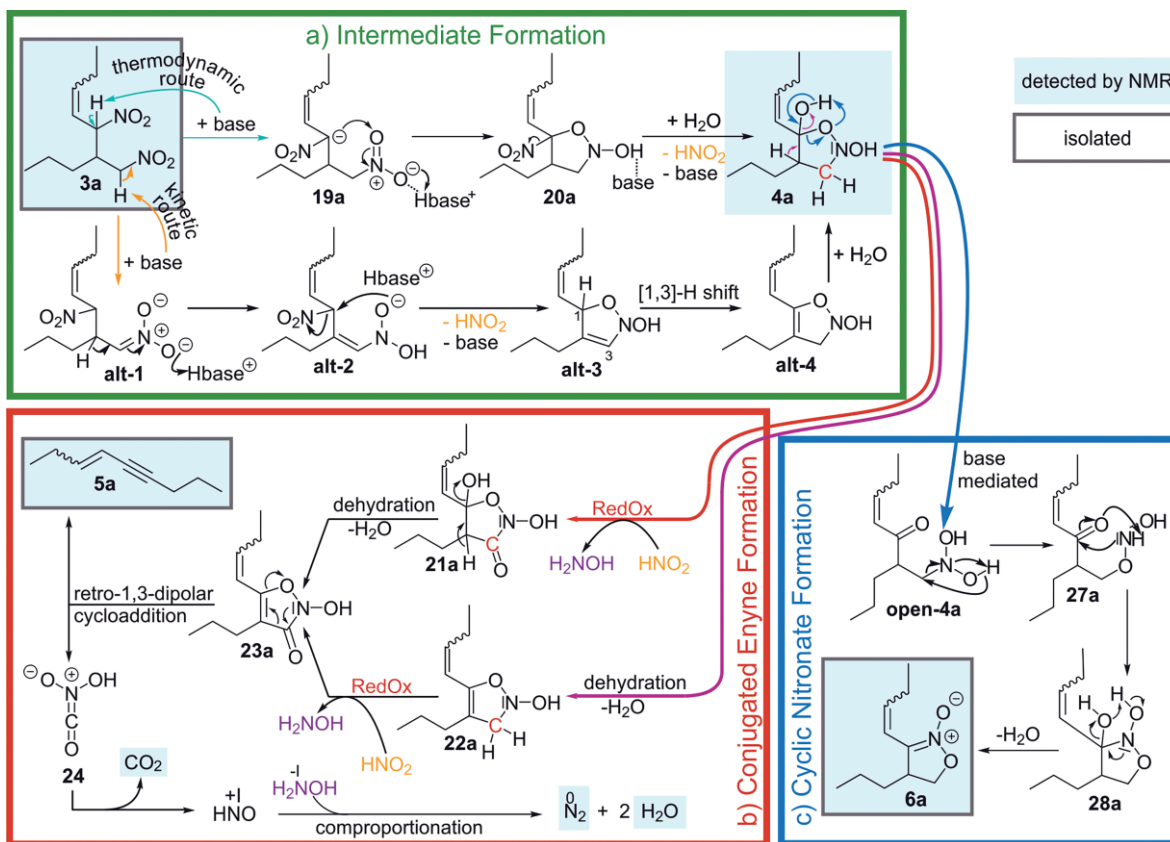
While, selectivity issues could be solved successfully (see above), the yields of both enynes **5** and nitronates **6** have remained limited so far due to the well-known polymerization

problems connected with nitroalkenes.^[27,49] This polymerization was evident from mass spectrometry (electrospray ionisation) throughout a one-pot reaction of **1a** with DBU revealing molecular ion peaks with *m/z* ratios higher than 800 (see Table 3 in SI). Furthermore, in the NMR spectra, the sum over all ¹H- signals belonging to the combined enyne and nitronate mechanism decreased in the ongoing reaction. Despite, several efforts including various bases, acidic additives, concentrations and temperatures, so far we have not been able to suppress effectively this detrimental polymerisation process. Nevertheless, in other reactions involving nitroalkenes such polymerisation processes could be successfully controlled.^[49] Thus, we are confident that the broad community of synthetic chemists working in the field of catalysis will find a way to raise the yields of this promising organocatalytic method to build up triple bonds in conjugated enynes.

Summary of Mechanistic Proposal and Conclusion

The first comprehensive mechanistic proposal of the combined metal-free route to conjugated enynes **5** and cyclic nitronates **6** is depicted in Scheme 5. Starting from nitroalkene dimers **3** NMR reaction profiles reveal a base initiated reaction to an isoxazolidine-2,5-diol derivative as intermediate **4** (see Scheme 5a). The unusual structure of this intermediate was corroborated by various NMR experiments including ¹⁵N labelling and theoretical calculations. Furthermore, NMR reaction profiles revealed **4** as central linking intermediate followed by separated pathways to enynes **5** (see Scheme 5b) and nitronates **6** (see Scheme 5c). While the enyne formation can proceed at both medium and high pH values, effective nitronate formation required basic conditions opening up an effective control of the product distribution. The unusual buildup of the triple bond out of a single bond in the enyne pathway is proposed to proceed via a combination of oxidation, dehydration and retro-1,3-dipolar cycloaddition. Theoretical calculations suggested the oxidation of intermediate **4a** as first step in the formation of **23a** under basic conditions. With acidic additives, both oxidation to **21a** and dehydration to **22a** may compete as first steps. The thereby generated unsaturated isoxazolidinone ring in **23a** is proposed to fragment via a retro-1,3-dipolar cycloaddition into conjugated enyne **5** and an oxidized nitronate **24**. This mechanistic proposal is corroborated by the experimentally detected byproducts N₂, CO₂ and H₂O. CO₂ and HNO may originate from the decomposition of **24**. HNO further compropionates with H₂NOH to the detected N₂ and H₂O. In the pathway towards cyclic nitronate **6** (Scheme 5c), theoretical calculations propose intramolecular rearrangements over open chain intermediates **open-4a** and **27a** to achieve the required change in heteroatom connectivity from **4** to **6**. The results of various reaction conditions corroborated the mechanism presented in Scheme 5. For example the addition of acids accelerated the formation of enynes **5** and suppressed nitronates nearly completely. In contrast, strong bases clearly facilitated the formation of nitronates **6**.

While mechanistic and selectivity issues were solved and high yields up to 84 % could be achieved for nitronates, only



Scheme 5. Overview of the proposed mechanism to conjugated enynes **5** and cyclic nitronates **6** shown for the nitropentene-derived dimer **3a**: a) formation of the central linking intermediate **4a** via two possible routes of base induced cyclizations; b) enyne pathway via a combination of oxidation, dehydration and retro-1,3-dipolar cycloaddition; c) nitronate formation via base mediated intramolecular reorganization of nitrogen and oxygen atoms. Blue boxes highlight the NMR-detected, gray frames the isolated compounds.

medium to good yields (< 57 %) were obtained for enynes, due to polymerization pathways well known for nitroalkenes. Nevertheless, we are confident that our mechanistic investigations have laid a groundwork for further improvements of this highly valuable, combined metal-free route to conjugated enynes and cyclic nitronates. Further, we hope that our results pave the way for further developments of organocatalytic or metal-free formations of conjugated enynes.

Experimental Section

NMR spectroscopic experiments were performed on a Bruker Avance III HD 400 MHz spectrometer, equipped with 5 mm BBO BB-¹H/D probe head with Z-Gradients, a Bruker Avance III HD 600 MHz spectrometer, equipped with a 5 mm TBI ¹H/¹⁹F and a Bruker Avance III 600 MHz equipped with a CryoProbe™ Prodigy. Chemical shifts δ in ppm are referenced on residual solvent signals or on internal standards. For NMR measurements employing standard NMR solvents 5 mm NMR tubes were used. NMR-reaction kinetics were performed using tetramethylsilane (TMS) or octamethylcyclotetrasiloxane (OMS) as internal standard. The samples for NMR-reaction monitoring were prepared from stock solutions of the respective reagents and reactants. For starting points ($t = 0$) spectra of the samples lacking the base were recorded. Afterwards, the base was added, and the reaction was monitored by NMR spectroscopy. High-resolution mass spectra (HRMS) were obtained on a Jeol

AccuTOF GCX instrument with an EI and a LIFDI source and on an Agilent Q-TOF 6540 UHD with an ESI source.

Nitroalkenes **1a**, **1a**¹³C and **1a**¹⁵N were synthesized following a literature procedure.^[50]

General Procedure for the Synthesis of Homo-Dimers: Nitroalkene **1** (1 mmol) and L-proline (1 mmol) were mixed in DMSO (10 mL). The reaction was left whilst stirring at room temperature overnight. The mixture was dissolved in water and extracted with dichloromethane. The combined organic phase was washed three times with a saturated solution of lithium chloride, dried with MgSO₄ and the solvent was evaporated. The product was purified by column chromatography (PE/DEE, 100:0–6:1).

5-Nitro-6-(nitromethyl)non-3-ene D1 (D2) (3a): 78 % yield. **3a Z:** ¹H NMR (600 MHz, [D₆]DMSO): δ = 5.91 (5.94) (m, 1 H), 5.56 (5.59) (m, 1 H), 5.55 (5.59) (m, 1 H), 4.63 (4.60/4.66) (m, 2 H), 2.91 (2.95) (m, 1 H), 2.16 (2.14) (m, 2 H), 1.31 (1.35/1.26) (m, 2 H), 1.30 (1.39) (m, 2 H), 0.95 (0.95) [t, J = 7.6 Hz (7.6 Hz), 3 H], 0.85 (0.85) [t, J = 7.1 Hz (7.1 Hz), 3 H] ppm. ¹³C NMR (600 MHz, [D₆]DMSO): δ = 141.7 (141.4), 120.0 (120.1), 85.0 (84.3), 74.9 (75.2), 39.2 (39.2), 29.4 (30.2), 20.4 (20.4), 18.6 (18.6), 13.5 (13.5), 13.2 (13.2) ppm. **3a E:** ¹H NMR (600 MHz, [D₆]DMSO): δ = 6.08 (6.03) [dt (dt), J = 15.3 Hz (15.3 Hz), 6.2 Hz (6.2 Hz) 1 H], 5.55 (5.69) [m (ddt) (J = 15.3 Hz, 9.7 Hz, 1.5 Hz), 1 H], 5.22 (5.25) [dd, J = 9.3 Hz, 8.6 Hz (9.3 Hz, 6.9 Hz), 1 H], \approx 4.62 (\approx 4.62) (m, 2 H), 2.92 (2.92) (m, 1 H), 2.04 (2.10) (m, 2 H), 1.60 (\approx 1.35) (m, 2 H), \approx 1.24 (\approx 1.28) (m, 2 H), 0.94 (1.05) (t, J = 7.6 Hz) (7.4 Hz, 3 H), 0.85 (0.85) (t, J = 7.1 Hz, 3 H) ppm. ¹³C NMR (600 MHz,

[D₆]DMSO): δ = 142.4 (142.2), 119.9 (119.8), 90.7 (89.5), 75.0 (75.6), \approx 39.2 (\approx 39.2), 30.8 (29.8), 24.4 (24.5), \approx 18.5 (\approx 18.5), \approx 13.5 (\approx 13.5), \approx 13.3 (\approx 13.3) ppm. HRMS (ESI): calcd. for C₁₀H₁₈N₂O₄ [M + H]⁺ 231.1339, found 231.1341.

General Procedure for the Synthesis of Hetero-Dimers: L-proline (0.2 mmol) and benzoic acid (0.2 mmol) were dissolved in DMSO (7 mL) at room temperature. Subsequently, the corresponding nitroalkenes (0.3 mmol each) were added. The solution was stirred for 24 h under atmospheric conditions. After the reaction was quenched by adding brine (10 mL) the reaction mixture was extracted 4 times with diethyl ether (10 mL each). The combined organic layers were washed 4 times with distilled water (10 mL each) and dried with magnesium sulfate. After evaporation of the solvent the raw product was purified by flash column chromatography (PE/EA = 9:1).

1-(5-Methyl-1,3-dinitrohex-4-en-2-yl)-2-nitrobenzene (3b):

Nitroalkenes (*E*)-3-methyl-1-nitrobut-1-ene and (*E*)-1-nitro-2-(2-nitrovinyl)benzene were applied as starting material. 24 % yield. ¹H NMR (400 MHz, [D₆]DMSO): δ = 8.09 (7.89) [d (d), *J* = 7.9 Hz (7.9 Hz)], 7.94 (7.94) (dd, *J* = 8.1 Hz, 1.2 Hz), 7.78 (7.78) (ddd, *J* = 7.8 Hz, 7.8 Hz, 1.1 Hz), 7.59 (7.59) (ddd, *J* = 7.8 Hz, 7.8 Hz, 1.2 Hz), 5.90 (6.03) [dd (dd), *J* = 9.9 Hz, 9.9 Hz (10.1 Hz, 10.1 Hz)], 5.44 (5.29) [dq (dq), *J* = 9.7 Hz, 1.3 Hz, 1.3 Hz (10-Hz, 1.3 Hz, 1.3 Hz)], 5.08 (5.22) [dd (dd), *J* = 13.8 Hz, 8.6 Hz (14.4 Hz, 10.3 Hz)], 4.96 (5.08) [dd (m), *J* = 13.8 Hz, 5.5 Hz], 4.79 (4.88) [ddd (ddd), *J* = 9.8 Hz, 8.7 Hz, 5.4 Hz (9.9 Hz, 9.9 Hz, 4.4 Hz)], 1.82 (1.59) [d (d), *J* = 1.1 Hz (1.2 Hz)], 1.79 (1.53) [d (d), *J* = 1.0 Hz (1.1 Hz)] ppm. ¹³C NMR (400 MHz, [D₆]DMSO): δ = 149.9 (150.3), 146.3 (146.4), 133.3 (133.3), 129.6 (129.6), 129.4 (129.1), 129.1 (129.0), 124.8 (124.8), 118.5 (116.6), 86.8 (85.3), 75.9 (76.7), 40.5 (39.7), 25.4 (25.1), 18.4 (18.1) ppm. HRMS (ESI): calcd. for C₁₃H₁₅N₃O₆ [M + Na]⁺ 332.0853, found 332.0855.

1-Methoxy-2-(5-methyl-1,3-dinitrohex-4-en-2-yl)benzene (3c):

Nitroalkenes (*E*)-3-methyl-1-nitrobut-1-ene and 1-methoxy-2-[(*E*)-2-nitrovinyl]benzene were applied as starting material. 24 % yield. ¹H NMR (400 MHz, [D₆]DMSO): δ = 7.31 (7.31) (dd, *J* = 7.5 Hz, 1.7 Hz, 1 H), 7.29 (7.29) (ddd, *J* = 7.9 Hz, 7.9 Hz, 1.6 Hz, 1 H), 7.03 (7.00) [dd (dd), *J* = 8.3 Hz, 0.7 Hz (8.2 Hz, 0.7 Hz), 1 H], 6.91 (6.91) (ddd, *J* = 7.4 Hz, 7.4 Hz, 1.0 Hz, 1 H), 5.87 (5.82) [dd (dd), *J* = 10.2 Hz, 10.2 Hz (9.9 Hz, 9.9 Hz), 1 H], 5.46 (5.19) [dq (dq), *J* = 9.9 Hz, 1.4 Hz, 1.4 Hz (9.9 Hz, 1.4 Hz, 1.4 Hz), 1 H], 4.89/4.80 (5.11/4.91) [dd/dd (dd), *J* = 13.4 Hz, 8.8 Hz/13.4 Hz, 5.6 Hz (13.3 Hz, 10.1 Hz), 2 H], 4.40 (4.50) [ddd (ddd), *J* = 10.2 Hz, 8.8 Hz, 5.7 Hz (9.9 Hz, 9.9 Hz, 4.7 Hz), 1 H], 3.83 (3.81) [s (s), 3 H] 1.79 (1.55) [d (d), *J* = 1.4 Hz (1.4 Hz), 3 H], 1.79 (1.53) [d (d), *J* = 1.4 Hz (1.3 Hz), 3 H] ppm. ¹³C NMR (400 MHz, [D₆]DMSO): δ = 149.9 (150.3), 145.0 (142.7), 129.6 (129.6), 129.4 (129.4), 122.7 (122.4), 120.6 (120.6), 117.1 (117.3), 111.7 (111.4), 86.0 (85.5), 75.5 (75.8), 55.7 (55.6), 42.2 (41.3), 25.4 (25.1), 18.3 (17.8) ppm. HRMS (ESI): calcd. for C₁₄H₁₈N₂O₅ [M + Na]⁺ 317.1108, found 317.1112.

For scope and syntheses of conjugated enynes and cyclic nitronates see Supporting Information.

Computational Details: For the calculation, a smaller model of dimer **3a** was employed. The *n*-propyl group and the terminal ethyl group connected with the double bond were substituted by a methyl group. All structures were optimized at M06-2X/def2-SVP level of theory using empirical dispersion D3 in continuum of DMF (CPCM).^[51-53] Thermochemical correction was performed at the same level of theory as the geometry optimization. Single point calculations were carried out at PWPB95-D3/def2TZVPP level of theory.^[54] The software used for the geometry optimization and frequency analysis was Gaussian09 version D.01.^[55] For the single

points, ORCA 4.0.1 was employed.^[56] For further details see Supporting Information.

Acknowledgments

We would like to thank the German Science Foundation (DFG, GS 13/3-1 and GS 13/4-1) for financial support. We regret that Dr. Markus Schmid refused to be Co-author of this manuscript and preferred to be cited in the given way. Nevertheless, we would like to thank him for the initialization of this project detecting first this unprecedented enyne formation.

Keywords: NMR spectroscopy · Enynes · Nitronates · Reaction mechanisms · Theoretical calculations

[1] M. Konishi, H. Ohkuma, K. Matsumoto, T. Tsuno, H. Kamei, T. Miyaki, T. Oki, H. Kawaguchi, G. D. Vanduyne, J. Clardy, *J. Antibiot.* **1989**, *42*, 1449–1452.
 [2] A. Stuetz, G. Petranyi, *J. Med. Chem.* **1984**, *27*, 1539–1543.
 [3] D. E. Rudisill, L. A. Castonguay, J. K. Stille, *Tetrahedron Lett.* **1988**, *29*, 1509–1512.
 [4] J. R. Frost, C. M. Pearson, T. N. Snaddon, R. A. Booth, R. M. Turner, J. Gold, D. M. Shaw, M. J. Gaunt, S. V. Ley, *Chem. Eur. J.* **2015**, *21*, 13261–13277.
 [5] T. Masaoka, Y. Hasegawa, T. Ueda, T. Takubo, H. Shibata, H. Nakamura, N. Tatsumi, J. Yoshitake, N. Senda, *Eur. J. Cancer* **1976**, *12*, 143–149.
 [6] B. M. Trost, L. Li, S. D. Guile, *J. Am. Chem. Soc.* **1992**, *114*, 8745–8747.
 [7] B. M. Trost, L. S. Chupak, T. Lübbbers, *J. Am. Chem. Soc.* **1998**, *120*, 1732–1740.
 [8] K. Karthikeyan, T. Veenus Seelan, K. G. Lalitha, P. T. Perumal, *Bioorg. Med. Chem. Lett.* **2009**, *19*, 3370–3373.
 [9] M. C. Pirrung, L. N. Tumey, C. R. H. Raetz, J. E. Jackman, K. Snehaltha, A. L. McClerren, C. A. Fierke, S. L. Gantt, K. M. Rusche, *J. Med. Chem.* **2002**, *45*, 4359–4370.
 [10] R. Maurya, P. Gupta, G. Ahmad, D. K. Yadav, K. Chand, A. B. Singh, A. K. Tamrakar, A. K. Srivastava, *Med. Chem. Res.* **2008**, *17*, 123–136.
 [11] H. Jiang, P. Elsner, K. Jensen, A. Falcicchio, V. Marcos, K. A. Jørgensen, *Angew. Chem. Int. Ed.* **2009**, *48*, 6844–6848; *Angew. Chem.* **2009**, *121*, 6976.
 [12] Y. Hatanaka, K. Matsui, T. Hiyama, *Tetrahedron Lett.* **1989**, *30*, 2403–2406.
 [13] Y. Hatanaka, T. Hiyama, *J. Org. Chem.* **1988**, *53*, 918–920.
 [14] B. P. Andreini, A. Carpita, R. Rossi, B. Scamuzzi, *Tetrahedron* **1989**, *45*, 5621–5640.
 [15] L.-X. Shao, M. Shi, *J. Org. Chem.* **2005**, *70*, 8635–8637.
 [16] D. Saha, T. Chatterjee, M. Mukherjee, B. C. Ranu, *J. Org. Chem.* **2012**, *77*, 9379–9383.
 [17] N. Miyaoura, K. Yamada, A. Suzuki, *Tetrahedron Lett.* **1979**, *20*, 3437–3440.
 [18] P.-F. Li, H.-L. Wang, J. Qu, *J. Org. Chem.* **2014**, *79*, 3955–3962.
 [19] H. Feuer, *Nitrile Oxides, Nitrones, and Nitronates in Organic Synthesis* John Wiley & Sons, **2008**.
 [20] J. M. Robinson, S. F. Tlais, J. Fong, R. L. Danheiser, *Tetrahedron* **2011**, *67*, 9890–9898.
 [21] M. Uchiyama, H. Ozawa, K. Takuma, Y. Matsumoto, M. Yonehara, K. Hiroya, T. Sakamoto, *Org. Lett.* **2006**, *8*, 5517–5520.
 [22] L. Anastasia, C. Xu, E. Negishi, *Tetrahedron Lett.* **2002**, *43*, 5673–5676.
 [23] V. Komanduri, M. J. Krische, *J. Am. Chem. Soc.* **2006**, *128*, 16448–16449.
 [24] Y.-T. Hong, C.-W. Cho, E. Skucas, M. J. Krische, *Org. Lett.* **2007**, *9*, 3745–3748.
 [25] G. Gervasio, P. J. King, D. Marabello, E. Sappa, *Inorg. Chim. Acta* **2003**, *350*, 215–244.
 [26] M. B. Schmid, *NMR Spectroscopic Investigations on Aminocatalysis: Catalysis and Intermediates, Conformations and Mechanisms* Dissertation, **2011**.
 [27] P. Shanbhag, P. R. Nareddy, M. Dadwal, S. M. Mobin, I. N. N. Namboothiri, *Org. Biomol. Chem.* **2010**, *8*, 4867–4873.
 [28] K. Kaur, I. N. N. Namboothiri, *Chimia* **2012**, *66*, 913–920.
 [29] D. Nair, T. Kumar, I. Namboothiri, *Synlett* **2016**, *27*, 2425–2442.

- [30] F. Ravalico, S. L. James, J. S. Vyle, *Green Chem.* **2011**, *13*, 1778–1783.
- [31] R. L. Benoit, D. Lefebvre, M. Fréchet, *Can. J. Chem.* **1987**, *65*, 996–1001.
- [32] P. Roose, K. Eller, E. Henkes, R. Rossbacher, H. Höke, in *Ullmann's Encycl. Ind. Chem.*, Wiley-VCH Verlag GmbH & Co. KGaA, Weinheim, Germany, **2015**, pp. 1–55.
- [33] I. M. Kolthoff, M. K. Chantooni, S. Bhowmik, *J. Am. Chem. Soc.* **1968**, *90*, 23–28.
- [34] W. M. Haynes, *CRC Handbook of Chemistry and Physics*, 97th Edition, CRC Press, Boca Raton, **2016**.
- [35] J. Jover, R. Bosque, J. Sales, *QSAR Comb. Sci.* **2008**, *27*, 563–581.
- [36] Z. Shi, B. Tan, W. W. Y. Leong, X. Zeng, M. Lu, G. Zhong, *Org. Lett.* **2010**, *12*, 5402–5405.
- [37] M. B. Schmid, K. Zeitler, R. M. Gschwind, *Chem. Eur. J.* **2012**, *18*, 3362–3370.
- [38] C. H. Bradley, G. E. Hawkes, E. W. Randall, J. D. Roberts, *J. Am. Chem. Soc.* **1975**, *97*, 1958–1959.
- [39] J. H. Dymond, *J. Phys. Chem.* **1967**, *71*, 1829–1831.
- [40] J. B. Lambert, G. Binsch, J. D. Roberts, *Proc. Natl. Acad. Sci. USA* **1964**, *51*, 735–737.
- [41] L. Kurti, B. Czako, *Strategic Applications of Named Reactions in Organic Synthesis* Elsevier, **2005**.
- [42] R. Ballini, G. Bosica, D. Fiorini, M. Petrini, *Tetrahedron Lett.* **2002**, *43*, 5233–5235.
- [43] M. Kinugasa, S. Hashimoto, *J. Chem. Soc., Chem. Commun.* **1972**, *4*, 466–467.
- [44] M. Miura, M. Enna, K. Okuro, M. Nomura, *J. Org. Chem.* **1995**, *60*, 4999–5004.
- [45] F. T. Bonner, M. N. Hughes, *Comments Inorg. Chem.* **1988**, *7*, 215–234.
- [46] F. Doctorovich, P. J. Farmer, M. Marti, *The Chemistry and Biology of Nitroxyl (HNO)*, Elsevier, **2016**.
- [47] S. Berger, S. Braun, H.-O. Kalinowski, *NMR-Spektroskopie von Nichtmetallen*, Georg Thieme Verlag, Stuttgart, **1993**.
- [48] L. V. Saloutina, E. V. Tretyakov, P. A. Slepukhin, V. I. Saloutin, O. N. Chupakhin, *J. Heterocycl. Chem.* **2017**, *54*, 1887–1890.
- [49] V. Barbier, F. Couty, O. R. P. David, *Eur. J. Org. Chem.* **2015**, 3679–3688.
- [50] B. M. Trost, C. Müller, *J. Am. Chem. Soc.* **2008**, *130*, 2438–2439.
- [51] Y. Zhao, D. G. Truhlar, *Theor. Chem. Acc.* **2008**, *120*, 215–241.
- [52] S. Grimme, J. Antony, S. Ehrlich, H. Krieg, *J. Chem. Phys.* **2010**, *132*, 154104.
- [53] J. Tomasi, B. Mennucci, R. Cammi, *Chem. Rev.* **2005**, *105*, 2999–3093.
- [54] L. Goerigk, S. Grimme, *J. Chem. Theory Comput.* **2011**, *7*, 291–309.
- [55] M. J. Frisch, G. W. Trucks, H. B. Schlegel, G. E. Scuseria, M. A. Robb, J. R. Cheeseman, G. Scalmani, V. Barone, B. Mennucci, G. A. Petersson, H. Nakatsuji, M. Caricato, X. Li, H. P. Hratchian, A. F. Izmaylov, J. Bloino, G. Zheng, J. L. Sonnenberg, M. Hada, M. Ehara, K. Toyota, R. Fukuda, J. Hasegawa, M. Ishida, T. Nakajima, Y. Honda, O. Kitao, H. Nakai, T. Vreven, J. A. Montgomery Jr., J. E. Peralta, F. Ogliaro, M. Bearpark, J. J. Heyd, E. Brothers, K. N. Kudin, V. N. Staroverov, R. Kobayashi, J. Normand, K. Raghavachari, A. Rendell, J. C. Burant, S. S. Iyengar, J. Tomasi, M. Cossi, N. Rega, J. M. Millam, M. Klene, J. E. Knox, J. B. Cross, V. Bakken, C. Adamo, J. Jaramillo, R. Gomperts, R. E. Stratmann, O. Yazyev, A. J. Austin, R. Cammi, C. Pomelli, J. W. Ochterski, R. L. Martin, K. Morokuma, V. G. Zakrzewski, G. A. Voth, P. Salvador, J. J. Dannenberg, S. Dapprich, A. D. Daniels, Ö. Farkas, J. B. Foresman, J. V. Ortiz, J. Cioslowski, D. J. Fox, *Gaussian 09, Revision D.01*, Gaussian, Inc., Wallingford CT, **2016**.
- [56] F. Neese, *Wiley Interdiscip. Rev.: Comput. Mol. Sci.* **2012**, *2*, 73–78.

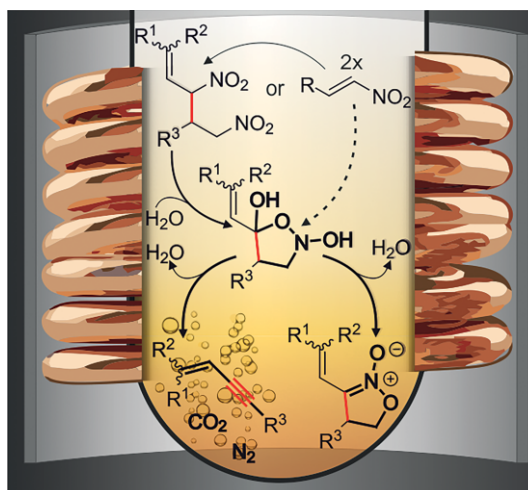
Received: July 23, 2018

Reaction Mechanism

V. Streitferdt, M. H. Haindl, J. Hioe,
F. Morana, P. Renzi, F. von Rekowski,
A. Zimmermann, M. Nardi,
K. Zeitler, R. M. G.* 1–11



Unprecedented Mechanism of an Organocatalytic Route to Conjugated Enynes with a Junction to Cyclic Nitronates



In situ NMR, isotope labelling, and theoretical calculations revealed an organocatalytic mechanism to conjugated enynes. This mild route to enynes proceeds through an unusual

build-up of the triple bond out of a single bond and provides a mechanistic junction to cyclic nitronates, which can be selectively switched by certain basic and acidic additives.

DOI: 10.1002/ejoc.201801153